

High-spin yrast cascade in  $^{60}\text{Ni}$ 

V. Potbhare

*Department of Physics, M. S. University, Baroda 390 002, India*

S. K. Sharma

*Department of Physics, Indian Institute of Technology Kanpur, Kanpur 208 016, India*

S. P. Pandya

*Physical Research Laboratory, Navrangpura, Ahmedabad 380 009, India*

(Received 13 April 1981)

The role played by the  $1g_{9/2}$  orbital vis-à-vis the structure of the recently observed high-spin yrast cascade in  $^{60}\text{Ni}$  is examined. The anomalous high-spin sequence is correctly reproduced. A number of electromagnetic transitions are predicted.

[ NUCLEAR STRUCTURE High-spin yrast levels in  $^{60}\text{Ni}$ : calculated energies, electromagnetic properties. Shell-model calculations in the  $(p_{3/2}p_{1/2}f_{5/2}g_{9/2})$  space. ]

Recently Kim *et al.*<sup>1</sup> have investigated experimentally the high-spin yrast spectrum in the nucleus  $^{60}\text{Ni}$  through the ( $\alpha$  particle or heavy ion, few nucleons and  $\gamma$ ) reactions. Their work has established a somewhat anomalous yrast spin sequence,  $9 \rightarrow 7 \rightarrow 6 \rightarrow 4^+ \rightarrow 2^+ \rightarrow 0^+$ . Similar yrast sequences (with  $J_{\text{max}} = 7$ ) have also been reported in the nuclei  $^{58}\text{Ni}$  and  $^{62}\text{Zn}$  by Ballini *et al.*<sup>2</sup> and Bruandet *et al.*,<sup>3</sup> respectively.

As pointed out by Kim *et al.*, a lack of reliable theoretical calculations has hindered any interpretation of the observed yrast schemes so far. A large number of shell model calculations<sup>4</sup> have earlier been carried out for  $^{60}\text{Ni}$  with the restriction that the four extra-core neutrons outside the  $^{56}\text{Ni}$  core be confined to only the  $p_{1/2}$ ,  $p_{3/2}$ , and  $f_{5/2}$  orbitals. However, to have  $J \geq 7$  it is necessary to open the core or include the  $g_{9/2}$  orbit.

Calculations have, in fact, in the recent past also been attempted by Jaffrin,<sup>5</sup> Shimizu and Arima,<sup>6</sup> and Parikh<sup>7</sup> with a view to incorporate the former effect. An important common feature of these attempts was the prediction of rather low excitation energies (4–5 MeV) of states with  $J^\pi = 8^+$ ,  $10^+$  in doubly even Ni isotopes. Significantly enough, however, the recent experiments<sup>1,2</sup> in  $^{58,60}\text{Ni}$  fail to show such states up to at least 7 MeV excitation in the yrast spectrum.

The failure of the earlier attempts<sup>5–7</sup> is not par-

ticularly surprising. A number of recent experiments have also cast doubts, although somewhat indirectly, on the adequacy of the configuration space employed in Refs. 5 and 7. Whereas Couch *et al.*,<sup>8</sup> as well as von Ehrenstein and Schiffer,<sup>9</sup> have found no firm evidence of  $1f_{7/2}$  holes in the nuclei in the Ni region (with  $A = 62–64$ ) from stripping experiments, McIntyre,<sup>10</sup> as well as Bettigeri *et al.*,<sup>11</sup> presented evidence from single nucleon pickup experiments that the  $g_{9/2}$  configuration does exist in their ground states with substantial particle occupation numbers ( $\sim 0.8$ ).

In this paper we report for the first time an exact shell model study of the high-spin states in  $^{60}\text{Ni}$  employing a valence space dictated by the above-mentioned considerations. Our space includes explicitly the  $g_{9/2}$  orbit at the expense of an omission of the  $f_{7/2}$  orbit. The relevant effective two-body interaction that we have employed is a renormalized  $G$  matrix due to Kuo<sup>12</sup> which is the sum of  $G_{\text{bare}}$ ,  $G_{3p-1h}$ , and  $G_{2p-2h}$  in the  $^{56}\text{Ni}$  core. The single-particle energies we have taken are (in MeV):  $e(p_{3/2}) = 0.0$ ,  $e(p_{1/2}) = 1.08$ ,  $e(f_{5/2}) = 0.78$ , and  $e(g_{9/2}) = 3.50$ .

In Fig. 1 we present a comparison of the calculated and experimental spectra. Our main aim here is to study the structure of the high-spin yrast states. However, for the calculation of these levels to be of some reliability, it is important to see whether it

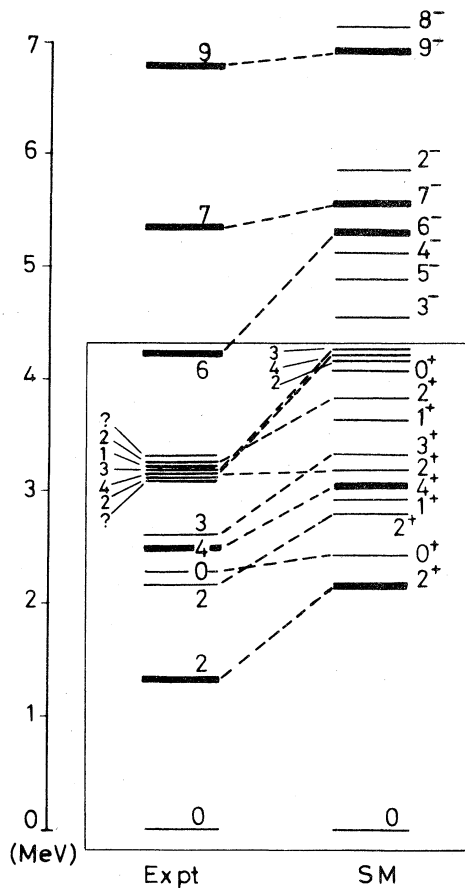


FIG. 1. A comparison between the observed and calculated level schemes. Due to the rapid increase in level density, only the yrast levels above 3.25 MeV in the experimental spectrum and only the negative parity levels above 4.25 MeV in the calculated spectrum are shown.

gives acceptable detailed agreement for the low-lying parts of the spectrum. From the figure (the portion inside the rectangle) one observes that this is indeed so.

Considering next the high-spin yrast spectrum, the present calculation is seen to be quite successful in explaining the observed anomalous spin sequence  $9 \rightarrow 7 \rightarrow 6 \rightarrow 4 \rightarrow 2 \rightarrow 0$ . The present calculation allows us to make unambiguous parity assignments of all the members of the observed yrast cascade except the  $J = 6$  state at 4.242 MeV. This is due to the near-degeneracy of the  $6^+$  and  $6^-$  states in the calculated spectrum. The  $J^\pi = 6^+$  state (not shown in Fig. 1) lies just 0.08 MeV above the yrast  $J^\pi = 6^-$  state. However, as we will discuss a little later, identifying the parity of the  $J = 6$  yrast level should not be too difficult if the half-life measurements we suggest here are carried out. Our assign-

ment of a negative parity to the observed  $J = 7$  state at 5.345 MeV is also consistent with the recent investigations of Bruandet *et al.*<sup>3</sup>

In Table I we display the dominant configurations entering into the wave functions of the yrast states. An important thing to note here is the non-collective nature of these states; just 4–5 configurations exhaust more than 85% of the strength of the complete wave function.

We move now to a discussion of electromagnetic observables. In Table II we have given the reduced transition probabilities for various possible electromagnetic transitions as well as the static quadrupole and magnetic moments for various yrast states. So far only the  $B(E2, 2 \rightarrow 0)$  has been experimentally measured.<sup>13</sup> In the framework of the present shell model calculation, we require an effective charge  $e = 1.73$  for the neutrons in  $^{60}\text{Ni}$  in order to match the observed and the computed values for the  $(2 \rightarrow 0)$  transitions. The effective charge thus obtained has then been used to compute the results presented in Table II.

A striking feature of our results for the static moments of the yrast states (see column 6 of Table II) is that they indicate a distinct and systematic shape transition along the yrast cascade. If we write<sup>14</sup> the wave function of a yrast state as the product of a deformed intrinsic state times an element of the rotation matrix  $D_{KM}^J(\theta, \phi)$ , i.e.,

$$\psi_M^J = D_{KM}^J \chi_K, \quad (1)$$

then the static quadrupole moment  $Q(J)$  can be related to the quadrupole moment of the intrinsic state ( $Q_0$ ) through

$$Q(J) = \frac{3K^2 - J(J+1)}{(J+1)(2J+3)} Q_0. \quad (2)$$

Assuming this prescription, it is seen that whereas the computed value of the quadrupole moment for the  $J^\pi = 2^+$  state suggests that it can be regarded as arising from a  $K = 0$ , oblate intrinsic state, the quadrupole moment values for the  $J > 2$  yrast states are consistent with their ( $K = 0$ ) prolate character. The fact that the  $B(E2, 4^+ \rightarrow 2^+)$  value is hindered roughly by a factor of 2 compared to the  $B(E2, 2^+ \rightarrow 0^+)$  value also emphasizes a sudden structural change at  $J = 2$ . It is worth mentioning here that, in the present model, the predictions involving ratios of the  $BE2$  values as well as the static moments do not depend on the choice of the effective charge. The latter is just a scale factor here since our valence space involves only neutrons. Incidentally, a shape transition quite similar to the one

TABLE I. Wave functions and energies  $E$  (experimental as well as theoretical) for the high-spin yrast cascade in  $^{60}\text{Ni}$ . The subscripts appearing on the wave functions components indicate the  $2j$  value of the single-particle orbital. The numbers in the parentheses indicate the seniority of the state. Amplitudes in the range  $(-0.2, 0.2)$  have been omitted. The sizes of the relevant shell model matrices in each case are  $N \times N$ .

$J_{\text{yrast}}^{\pi}$	$N$	Wave function	$E$ (th)	$E$ (exp)
$0^+$	21	$0.58p_3^4(0) + 0.57p_3^2f_5^2(0) - 0.33p_3^2p_1^2(0)$ $0.26p_3^2g_9^2(0) + 0.24f_5^4(0) - 0.22f_5^2g_9^2(0)$	0.00	0.00
$2^+$	53	$0.66p_3^3p_1(2) + 0.36p_3^2(0)f_5^2(2)$ $+ 0.33p_3f_5g_9^2(2) + 0.26p_3^2p_1^2(2)$ $+ 0.25p_3^2f_5p_1(2) + 0.22p_3^2f_5^2(4)$	2.16	1.33
$4^+$	54	$0.81p_3^3f_5(2) + 0.43p_3f_5^3(2)$ $+ 0.26p_3f_5p_1^2(2) - 0.22p_3f_5g_9^2(2)$	3.05	2.51
$6^-$	46	$0.63p_3^2f_5g_9(2) + 0.62p_3^3g_9(2)$ $+ 0.30p_3p_1^2g_9(2)$	5.30	(4.26)
$6^+$	40	$0.96p_3^2f_5^2(4) - 0.24p_3f_5^3(4)$	5.38	(?)
$7^-$	34	$0.76p_3^2f_5g_9(2) + 0.48f_5^3g_9(2) +$ $0.29p_3^2p_1g_9(2) + 0.21f_5g_9^3(2)$	5.56	5.35
$9^-$	14	$0.86p_3^2f_5g_9(2) + 0.41p_3f_5p_1g_9(4)$	6.92	6.81

TABLE II. Electromagnetic properties of the members of the yrast cascade in  $^{60}\text{Ni}$ . The reduced transition probabilities are given in units of  $e^2\text{fm}^{2L}$  for EL and of  $\mu_N^2\text{fm}^{2L-2}$  for ML transitions.

$J_i^{\pi}$	$J_f^{\pi}$	$E$ (keV)	Type of transition (EL/ML)	$B$ (EL/ML)	$Q$ ( $J_i^{\pi}$ ) ( $e\text{fm}^2$ )	$\mu$ ( $J_i^{\pi}$ ) ( $\mu_N$ )
$2^+$	$0^+$	1332	$E2$	180.21	6.57	1.49
$4^+$	$2^+$	1172	$E2$	78.98	-7.83	2.82
$6^-$	$4^+$	1757	$M2$	610.98	-41.59	$-1.22 \times 10^{-1}$
$6^+$	$4^+$		$E2$	36.22	-16.28	4.72
$6^+$	$6^-$		$M2$	2.38		
$7^-$	$6^-$	1083	$E2$	3.11	-53.28	5.11
$7^-$	$6^+$	1083	$M1$	$2.30 \times 10^{-3}$		
			$E1$	0.00		
			$M2$	0.18		
$9^-$	$7^-$	1462	$E2$	114.11	-64.62	5.66

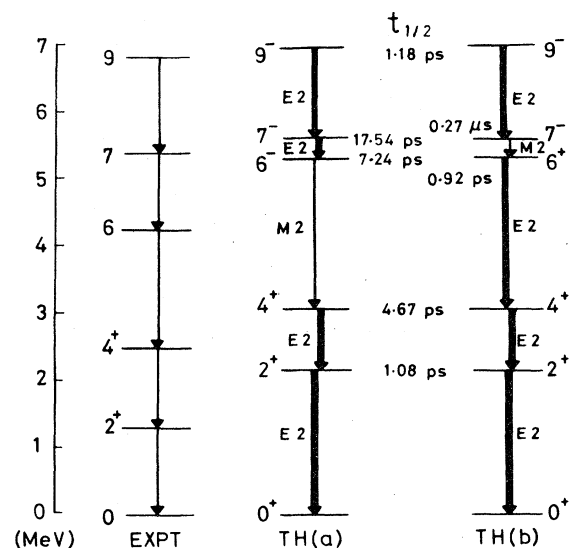


FIG. 2. Observed and theoretical decay schemes for the yrast levels in  $^{60}\text{Ni}$ . The two theoretical schemes correspond to the two different choices for the parity of the  $J = 6$  level at 4.242 MeV: (a) negative parity and (b) positive parity.

we predict here has recently been reported experimentally by Bendjaballah *et al.*<sup>15</sup> in the yrast band in  $^{56}\text{Fe}$ .

We now return to the question of the parity assignment for the  $J = 6$  level at 4.242 MeV. We chose for our calculations the energies for the single particle  $p_{3/2}$ ,  $p_{1/2}$ , and  $f_{5/2}$  states from the observed spectrum in  $^{57}\text{Ni}$ . However, the energy for the  $g_{9/2}$  orbit was somewhat empirically taken to be 3.50 MeV. From the present work, it turns out that although the overall features of the positive- and

negative- parity states separately are affected only marginally under a reasonable variation of the  $g_{9/2}$  energy, the  $(6^+ - 6^-)$  energy separation is almost linearly dependent on  $e(g_{9/2})$ . The observed yrast decay scheme does not presently rule out either of the two theoretical schemes presented in Fig. 2. We have presented here the half-life estimates corresponding to the two schemes. A remarkable difference between the two schemes lies in their predictions of the half-life values for the observed  $J = 7$  level at 5.345 MeV—whereas the value arising from the decay sequence (a) is about 17.5 psec, that resulting from the sequence (b) is about 0.27  $\mu\text{sec}$ , which is roughly 15 390 times longer. The identification of the correct yrast scheme through half-life as well as polarization measurements would not only be interesting in itself but would also help very much in ascertaining the position of the  $g_{9/2}$  orbit in  $^{57}\text{Ni}$  with good accuracy.

Summarizing, a reasonably successful microscopic description of the recently observed, anomalous high-spin yrast cascade in  $^{60}\text{Ni}$  can be given provided one considers an explicit inclusion of the  $g_{9/2}$  orbit in the valence space. A number of electromagnetic transitions have been predicted. The necessity of carrying out certain specific measurements in the context of making the present model more precise for  $^{60}\text{Ni}$ —as well as for a number of other nuclei in the  $A = 60-70$  mass region—is pointed out.

*Note added in proof:* After this paper was submitted, the recent experimental work of Moyat *et al.*<sup>16</sup> as well as Kearns *et al.*<sup>17</sup> was brought to our notice. The half-life measurements reported in these investigations are consistent with the theoretical decay sequence TH(b) presented here.

- <sup>1</sup>H. J. Kim *et al.*, Nucl. Phys. **A250**, 211 (1975).  
<sup>2</sup>R. Ballini *et al.*, Nucl. Phys. **A258**, 388 (1976).  
<sup>3</sup>J. F. Bruandet *et al.*, Z. Phys. **A279**, 69 (1976).  
<sup>4</sup>R. D. Lawson, M. H. McFarlane, and T. T. S. Kuo, Phys. Lett. **22**, 168 (1966); S. Cohen *et al.*, Phys. Rev. **160**, 903 (1967); N. Auerbach, Phys. Rev. **163**, 1203 (1967); E. A. Phillips and A. D. Jackson, Phys. Rev. **169**, 917 (1968); S. S. M. Wong, Nucl. Phys. **A159**, 235 (1970); P. W. M. Glaudemans, M. J. A. de Voigt, and E. F. M. Steffens, Nucl. Phys. **A198**, 609 (1972); J. E. Koops and P. W. M. Glaudemans, Nucl. Phys. (to be published).  
<sup>5</sup>A. Jaffrin, Phys. Lett. **32B**, 448 (1970).  
<sup>6</sup>K. Shimizu and A. Arima, Nucl. Phys. **A227**, 357 (1974).  
<sup>7</sup>J. K. Parikh, Phys. Rev. **C10**, 2568 (1974).

- <sup>8</sup>R. G. Couch *et al.*, Phys. Rev. **C2**, 149 (1970).  
<sup>9</sup>D. von Ehrenstein and J. P. Schiffer, Phys. Rev. **164**, 1374 (1967).  
<sup>10</sup>J. C. McIntyre, Phys. Rev. **152**, 1013 (1966).  
<sup>11</sup>M. G. Betigeri *et al.*, Nucl. Phys. **A171**, 401 (1971).  
<sup>12</sup>T. T. S. Kuo (private communications).  
<sup>13</sup>A. Christy and O. Hausser, Nucl. Data Tables **11**, 281 (1972).  
<sup>14</sup>G. Ripka, in *Advances in Nuclear Physics*, edited by M. Baranger and E. Vogt (Plenum, New York, 1968), Vol. 1.  
<sup>15</sup>N. Bendjaballah, J. Delaunay, T. Nomura, and H. J. Kim, Phys. Rev. Lett. **36**, 1536 (1976).  
<sup>16</sup>G. Moyat *et al.*, Nucl. Phys. **A318**, 236 (1979).  
<sup>17</sup>F. Kearns *et al.*, J. Phys. **G6**, 1131 (1980).